Quantifying the flux of $CaCO_3$ and organic carbon from the surface ocean using in situ measurements of O_2, N_2, pCO_2, and pH

Steven Emerson,[1] Christopher Sabine,[2] Meghan F. Cronin,[2] Richard Feely,[2] Sarah E. Cullison Gray,[3] and Mike DeGrandpre[3]

Received 22 July 2010; revised 11 March 2011; accepted 8 April 2011; published 16 July 2011.

[1] Ocean acidification from anthropogenic CO_2 has focused our attention on the importance of understanding the rates and mechanisms of $CaCO_3$ formation so that changes can be monitored and feedbacks predicted. We present a method for determining the rate of $CaCO_3$ production using in situ measureme nts of fCO_2 and pH in surface waters of the eastern subarctic Pacific Ocean. These quantities were determined on a surface mooring every 3 h for a period of about 9 months in 2007 at Ocean Station Papa (50°N, 145°W). We use the data in a simple surface ocean, mass balance model of dissolved inorganic carbon (DIC) and alkalinity (Alk) to constrain the $CaCO_3$: organic carbon (OC) production ratio to be approximately 0.5. A $CaCO_3$ production rate of 8 mmol $CaCO_3$ m^{-2} d^{-1} in the summer of 2007 (1.2 mol m^{-2} yr^{-1}) is derived by combining the $CaCO_3$: OC ratio with the a net organic carbon production rate (2.5 mol C m^{-2} yr^{-1}) determined from in situ measurements of oxygen and nitrogen gas concentrations measured on the same mooring (Emerson and Stump, 2010). Carbonate chemistry data from a meridional hydrographic section in this area in 2008 indicate that isopycnal surfaces that outcrop in the winter in the subarctic Pacific and deepen southward into the subtropics are a much stronger source for alkalinity than vertical mixing. This pathway has a high enough Alk:DIC ratio to support the $CaCO_3$:OC production rate implied by the fCO_2 and pH data.

Citation: Emerson, S., C. Sabine, M. F. Cronin, R. Feely, S. E. Cullison Gray, and M. DeGrandpre (2011), Quantifying the flux of $CaCO_3$ and organic carbon from the surface ocean using in situ measurements of O_2, N_2, pCO_2, and pH, *Global Biogeochem. Cycles*, *25*, GB3008, doi:10.1029/2010GB003924.

1. Introduction

[2] The $CaCO_3$: organic carbon (OC) mix of the particulate and dissolved material that exits the surface ocean strongly influences the effect of the biological pump on the fCO_2 of the atmosphere [e.g., *Broecker and Peng*, 1982; *Sarmiento and Gruber*, 2007; *Emerson and Hedges*, 2008]. This mixture also helps determine the depth at which the exported particulate organic matter degrades [*Klaas and Archer*, 2002; *Armstrong et al.*, 2002], which greatly influences the effectiveness of the marine carbon pump on atmospheric fCO_2 and deep ocean oxygen concentration [*Yamanaka and Tajika*, 1996; *Kwon et al.*, 2009]. Thus, changes in the formation rate of $CaCO_3$-containing algae in response to anthropogenic CO_2 addition to the atmosphere will cause a carbon cycle feedback that is presently difficult to predict.

[3] Global estimates of the formation rate of $CaCO_3$ in ocean surface waters are based primarily on interpretation of climatological distributions of alkalinity (Alk) and dissolved inorganic carbon (DIC) using seasonal changes in mixed-layer alkalinity [*Lee*, 2001] and calculation of vertical fluxes based on gradients in subsurface waters [*Sarmiento et al.*, 2002; *Moore et al.*, 2002; *Jin et al.*, 2006]. In addition, *Balch et al.* [2007] have interpreted satellite measurement of reflectance and color in terms of $CaCO_3$ standing stocks. Global $CaCO_3$ export rates derived from these methods range from 0.5 to 1.6 Gt C yr^{-1} (see *Jin et al.* [2006] and *Berelson et al.* [2007] for reviews). The fate of particulate $CaCO_3$ after it leaves the upper ocean has been determined by distinguishing the fraction of the measured water column alkalinity that can be attributed to $CaCO_3$ dissolution, TA* [*Feely et al.*, 2002], by sediment trap experiments [e.g., *Honjo et al.*, 1995; *Wong et al.*, 1999] and by sediment-water dissolution and burial measurements [*Hales and Emerson*, 1997; *Jahnke et al.*, 1994; *Berelson et al.*, 2007].

[4] This paper presents the results of the first successful long-term (9 month) autonomous in situ measurements of

[1]School of Oceanography, University of Washington, Seattle, Washington, USA.
[2]Pacific Marine Environmental Laboratory, NOAA, Seattle, Washington, USA.
[3]Department of Chemistry and Biochemistry, University of Montana, Missoula, Montana, USA.

0886-6236/11/2010GB003924

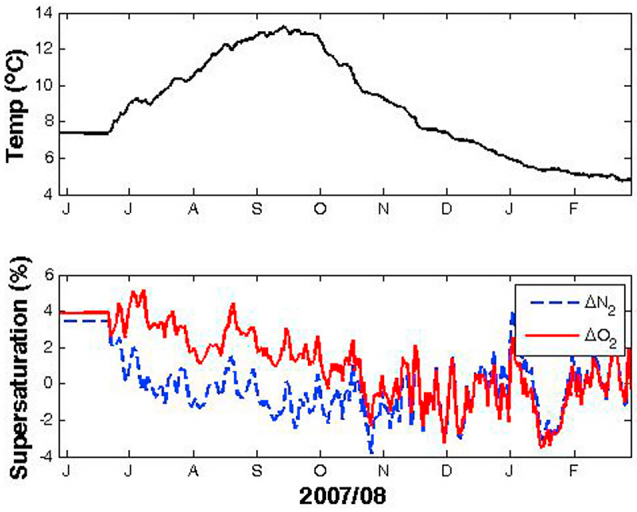

Figure 1. Changes in (a) temperature and (b) the degree of supersaturation of oxygen and nitrogen in the surface waters at Stn P (50°N and 145°W). Notice the evolution of the difference between O_2 and N_2 supersaturation between summer and winter. These data were used in a simple upper ocean model to determine the net biological O_2 production in a companion paper [*Emerson and Stump*, 2010].

both fCO_2 and pH in open ocean surface waters, and its interpretation in terms of the ratio of $CaCO_3$: OC production. We believe that this general method could be used to ground truth the rates of $CaCO_3$ production derived from GCMs and satellites. The work presented here is the companion to another paper [*Emerson and Stump*, 2010] in which in situ measurements of O_2 and N_2 from the same mooring deployment were interpreted in terms of net community production (NCP) of oxygen and organic matter. By combining these results with simultaneous measurements of fCO_2 and pH we constrain the $CaCO_3$: OC formation ratio to be about 0.5 and the $CaCO_3$ production rate to be ~8 mmol m^{-2} d^{-1} in the summer of 2007 in the subarctic Pacific Ocean. We show that the likely transport pathway for resupplying alkalinity removed from North Pacific surface waters is along isopycnal surfaces that plunge into deeper waters to the south rather than by vertical processes assumed in the earlier studies.

2. Setting and Methods

2.1. Station Papa

[5] The subarctic Pacific Ocean at Ocean Station Papa (hereafter Stn. P, located at 50°N, 145°W) is a region where precipitation and fresh water runoff from the continents exceeds evaporation leading to a layer of low-salinity water that caps a permanent halocline. There is a strong seasonality in temperature in surface waters (Figure 1a). In winter the Aleutian low is positioned in the Gulf of Alaska and brings winds that average 12 m s^{-1} which combine with cold temperatures (<6°C) to mix the surface layer to depths of the halocline at about 110 m. In summer the Aleutian low moves northward and wind speeds drop to an average of 7–8 m s^{-1} allowing the formation of a shallower thermocline and the mixed layer decreases to 25–30 m as the waters warm. Geostrophically driven surface currents in the subarctic region north of 42°N are characterized by cyclonic circulation in which the flow west of 140°W and south of 55°N is to the east [*Favorite et al.*, 1976], with a surface Ekman flow in the vicinity of Stn P to the southeast. In a classic interpretation of the hydrographic data from weather ships during the period of the 1950s and 1960s, *Tabata* [1961] showed that the salt balance in the region constrains upward advection across the halocline to an annually averaged value of 10–20 m yr^{-1}. This work and more recent studies [*Large et al.*, 1986; *Archer et al.*, 1993; *Large et al.*, 1994] demonstrated that a one dimensional heat and nutrient budget is pretty well closed in summer, but in the fall and winter horizontal fluxes become an important component of the transport.

[6] The macronutrients dissolved inorganic nitrogen (DIN) and dissolved inorganic phosphate (DIP) are above detection limits by traditional methods in surface waters of the high-latitude North Pacific Ocean year-round. *Wong et al.* [2002] demonstrated using 2 years of surface water sampling from container ships that NO_3^- levels drop from values of about 17 μmol kg^{-1} in winter to about 8 μmol kg^{-1} in August and September. These changes were interpreted along with Redfield stoichiometry (ΔC: ΔN = 6.6) to indicate a summertime carbon export from the mixed layer of ~19 mmol C m^{-2} d^{-1}. This result is very similar to that determined based on oxygen mass balance (17 mmol C m^{-2} d^{-1}) using in situ O_2 and N_2 measurements [*Emerson and Stump*, 2010]. The latter result was determined from a simple upper ocean model and in situ measurements of the degree of supersaturation of oxygen and nitrogen (see Figure 1b). Net biological oxygen production determined from these data is proportional to the difference in supersaturation between oxygen and nitrogen gas ($\Delta O_2 - \Delta N_2$), which is very large during summer and effectively non existent in winter. We used these data to suggest that almost all of the net biological carbon production in this area was in summer [*Emerson and Stump*, 2010], and our interpretation of the fCO_2 and pH data in this paper will also focus in the period of June-October 2007.

[7] A convenient aspect of studying the carbonate chemistry in the northeast subarctic Pacific is that Sta P has been the site of intensive studies of particle fluxes [*Wong et al.*, 1999; D. Timothy et al., The climatology and nature of settling particles in the subarctic northeast Pacific Ocean based on 24 years of sediment-trap flux, submitted to *Progress in Oceanography*, 2011], dissolved inorganic carbon changes [*Wong et al.*, 2002] and biological calcification [*Lipsen et al.*, 2007]. In the DISCUSSION section we evaluate the efficacy of our in situ measurements and model by comparing our results of net organic carbon and $CaCO_3$ production with those from previous observations.

2.2. Mooring Time Series Methods

[8] We report approximately 1 year of data from a heavily instrumented surface mooring deployed at Stn. P that started in June 2007 and now continues as a NOAA contribution to the global network of OceanSITES reference stations. The surface meteorological suite of sensors on the mooring included a Gill sonic anemometer that made a 2 min average of wind speed and direction measurements every 10 min.

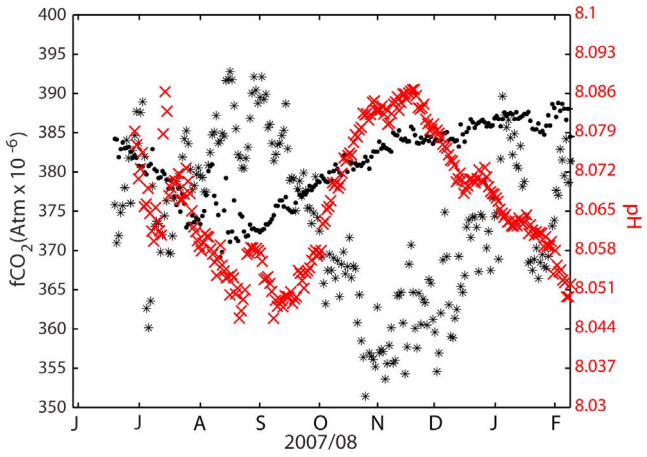

Figure 2. Surface water fCO_2 (dark asterisk), pH (red cross), and atmospheric fCO_2 (dark square) at Stn P from June 2007 till about February 2008. Daily averages are plotted from measurements every 3 h by in situ sensors on a surface mooring.

Surface ocean temperature and salinity were measured at 10 min intervals at 1 m, 5 m, 8 m, 10 m, 35 m, 45 m, (and 5 more depths down to 200 m), and at hourly intervals at 20 m. An hourly time series of the mixed-layer depth was computed by determining the depth at which the density was 0.2 kg m^{-3} larger than the 1 m surface value. Currents were measured every 20 min at 5 m and 35 m depths using Sontek acoustic Doppler current meters. Data from this project can be found on the Web at http://www.pmel.noaa.gov/stnP/.

[9] Measurements of oxygen and total gas tension at two meters depth were used to determine the concentrations of O_2 and N_2. These methods and data have been presented and interpreted previously [*Emerson and Stump*, 2010]. Here we focus on describing the utility of fCO_2 and pH measurements in determining the contribution of $CaCO_3$ formation to the local carbon cycle. (See *Cullison Gray et al.* [2011] for a more general evaluation of calculating inorganic carbon species from pH and fCO_2 measurements.)

[10] The mole fraction of carbon dioxide was measured at a depth of about one meter and in the atmosphere every 3 h using the NOAA/PMEL-built $MAPCO_2$ system. This system uses an automated bubble equilibrator-based gas collection system with an infrared gas analyzer (Li-820, Li-Cor Biogeosciences, Incorporated, Lincoln, Nebraska). The equilibrator is based on the design of *Friederich et al.* [1995]. Calibration is performed immediately prior to the atmospheric and surface ocean measurements using a CO_2 calibration span gas that has been compared to standards from NOAA/ESRL which are traceable to World Metrological Organization (WMO) references. System accuracy is estimated to be 1–2 ppm based on laboratory calibrations, field comparisons with underway CO_2 systems, and international intercomparison exercises. Data and diagnostic information are transmitted from the system to PMEL daily and posted on the Web in near-real time (http://www.pmel.noaa.gov/co2/moorings/papa/papa_main.htm).

[11] pH measurements were made every 3 h with a Sunburst Sensors automated pH sensor that was attached to the mooring bridle at a depth of about 2 m. Hydrogen ion concentrations are determined with this instrument spectrophotometrically using a sulphonephthalein indicator that develops a pH-dependent color [*Martz et al.*, 2003; *Seidel et al.*, 2008]. Because small samples are used and a rather short path length is necessary, the effect of the reagent addition on the in situ pH is determined by using a dye dilution curve and extrapolating the measured absorption readings to the values for zero added reagent. The method is precise to better than ±0.001 pH unit and accurate to ±0.002 pH units based on laboratory tests in which results of the in situ instrument were compared with those determined by hand on a laboratory spectrophotometer. Data from the instrument was recorded internally and downloaded when it was retrieved during buoy replacement (once each year).

2.3. Seawater Hydrography and Carbonate Chemistry

[12] We also present carbonate chemistry and hydrographic data from a University of Washington Student Cruise on the R. V. *Thompson* between Ocean Station P and Hawaii in August/September 2008 (TN224). The cruise track headed south from Stn P (145°W, 50°N) to 38°N, then jogged north to 45°N and 152°W where it again turned south and followed the meridional transect occupied previously by CLIVAR P16 along 152°W. (See *Howard et al.* [2010] for more information about the cruise.) Hydrographic stations were occupied every 2 degrees with sampling to depths of 1000–2000 m. Dissolved inorganic carbon (DIC) was analyzed by coulometry [*Johnson et al.*, 1998] and alkalinity by open-cell potentiometric titration [*Millero et al.*, 1998; *Dickson et al.*, 2003]. Certified reference materials [*Dickson et al.*, 2003] were used to validate accuracy of both methods. Duplicate analysis of reference materials and samples indicate a precision of ±2 μmol kg^{-1} and ±4 μeq kg^{-1} for DIC and Alk, respectively.

3. Results

3.1. Surface Ocean fCO_2 and pH Time Series

[13] Data from June 2007 to February 2008 (Figure 2) indicate seasonal changes of ~55 ppm for fCO_2 and ~0.04 pH units. Scatter around the daily averaged trends presented in Figure 2 is on the order of the errors reported above. The fCO_2 values are near atmospheric equilibrium (375–390) with slight supersaturation in summer and undersaturation in winter, which is similar to earlier seasonal fCO_2 data from this time series location [*Wong and Chan*, 1991]. The pH measurements follow a trend opposite to that of fCO_2. Data associated with each measurement indicated that the linearity in the trend of pH absorbance versus volume of added reagent during the dye dilution curves began to deteriorate (dropped below $r^2 = 0.99$) after November 2007 (~day 330). We do not interpret the pH data after this time because of uncertain accuracy. There is not a third measurement of the carbonate system from the same location and time for an independent check on the accuracy of these measurements. We will show, however, that the formation rate of $CaCO_3$ depends mainly on the observed changes in pH and fCO_2 rather than absolute values. Thus, small inaccuracies that could exist will not affect our conclusions. Drift in the pH data due to biofouling, however, could be a problem, and in

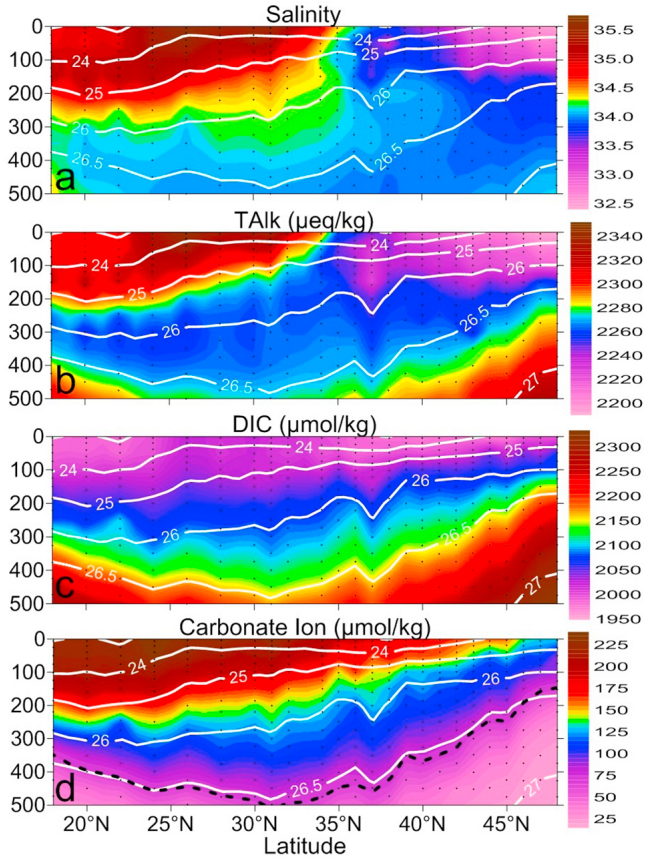

Figure 3. Sections of (a) salinity (color scale is in, ppt), (b) Alk (color scale is in, μeq kg^{-1}), (c) DIC (color scale is in μmol kg^{-1}) and (d) [CO_3^{2-}] (color scale, μmol kg^{-1}) as a function of depth (m) along 152°W from *Thompson* cruise TN224 (August/September 2008). Constant density surfaces are indicated by the white contour intervals. The dark, dashed line in Figure 3d is the depth of the aragonite saturation horizon ($\Omega_{arag.} = 1$).

current field studies we are determining Alk and DIC at each opportunity to empirically determine stability.

3.2. Hydrographic Data From TN224

[14] A section of the hydrographic data from the Student Cruise in 2008 is presented in Figure 3. Meridional trends along 152°W are shown as a function of depth and density. The low-salinity waters of the surface subarctic Pacific contrast the high-salinity waters in the subtropics (Figure 3a). Meridional trends in surface water alkalinity follow those of salinity much more closely than do DIC changes (Figures 3b and 3c) indicating the more conservative behavior of alkalinity [*Lee et al.*, 2006]. The carbonate ion concentration (Figure 3d) was calculated from DIC and Alkalinity using the apparent constants for the carbonate equilibria presented by *Lueker et al.* [2000]. The dashed line in Figure 3d indicates the saturation horizon for aragonite (aragonite is supersaturated above and undersaturated below) using the aragonite solubility product presented by *Mucci* [1983] and assuming calcium is a conservative ion in seawater and varies only with salinity. The saturation horizon follows $\sigma_\theta \sim 26.5$ which plunges from depths just below the euphotic zone at 50°N to between 400 and 500 m in the subtropics.

4. Discussion

4.1. Carbonate Equilibrium

[15] Changes in the pH and fCO_2 of surface seawater depend on temperature, salinity and reactions that alter dissolved inorganic carbon and total alkalinity. We demonstrate these effects on the data by calculating the carbonate ion concentration (Figure 4 and equation (1)) from measured pH and fCO_2. Chemical equilibrium constants used in the calculation are: the Henry's Law coefficient for CO_2 solubility in seawater (K_H, *Weiss* [1974]), and the values reported by *Lueker et al.* [2000] for the hydration of CO_2 to HCO_3^- (K_1') and the equilibrium between HCO_3^- and CO_3^{2-} (K_2'). *Lueker et al.* [2000] demonstrated that the dissociation constants determined by *Mehrbach et al.* [1973] interpreted on the "total hydrogen scale" give internally consistent results when combined with highly precise measurements of Alk, DIC and fCO_2 values below 500 micro atmospheres.

$$[CO_3^{2-}] = K_H K_1' K_2' \frac{fCO_2}{[H^+]^2} \quad (1)$$

Individual points in Figure 4 are carbonate ion concentrations determined from fCO_2, pH, T and S data. The line is the expected [CO_3^{2-}] change for constant values of DIC and Alk but varying T and S. The observed increase in [CO_3^{2-}] by 5–15 μmol kg^{-1} cannot be due to surface water temperature and salinity changes alone—it requires some combination of biological processes and gas exchange that alter dissolved inorganic carbon (and possibly alkalinity).

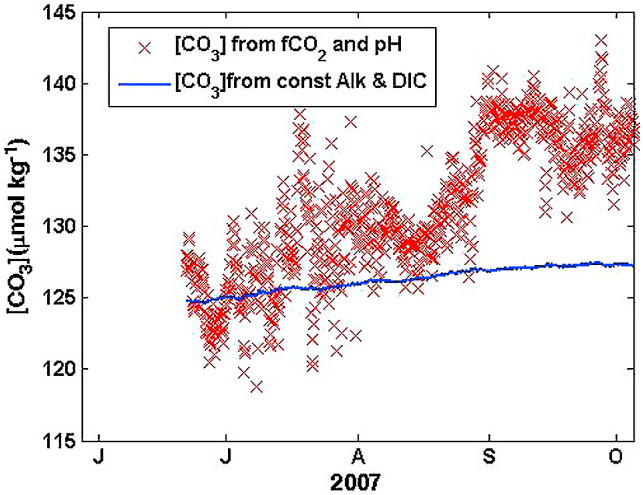

Figure 4. Carbonate ion concentrations (x) as a function of time in the surface ocean calculated from fCO_2, pH, T, and S using carbonate equilibria (see section 4.1). The line is the value calculated from carbonate equilibrium for constant Alk and DIC and the measured temperature and salinity. (Initial values are T = 7.04°C, S = 32.58, Alk = 2.373 meq kg^{-1}, and DIC = 2.204 mmol kg^{-1}).

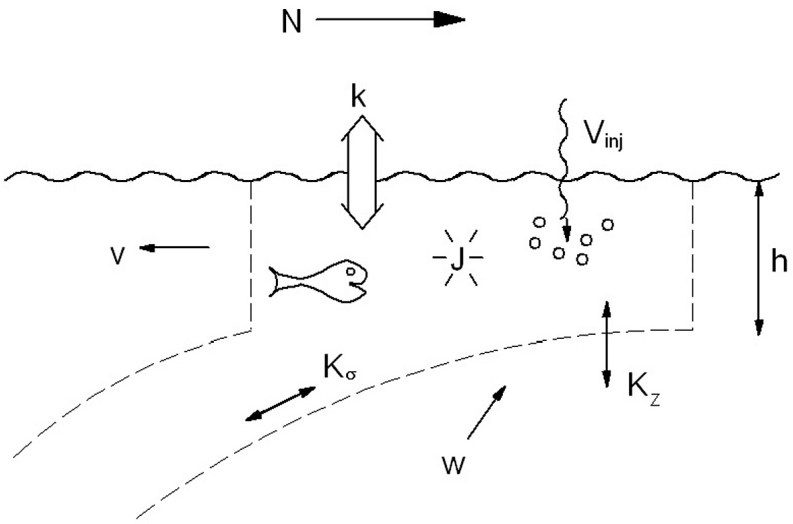

Figure 5. A schematic representation of the model used to determine net biological fluxes from the mixed layer at Stn P. Dashed lines represent constant density surfaces, and h is the mixed layer depth. J is the net biological production and export (equation (3)). Other symbols associated with arrows are mass transfer coefficients that appear in equations (4)–(8). They are the mass transfer coefficients for gas exchange, k (equation (4)), and bubble air injection, V_{inj} (equation (4)); advection velocities in both the horizontal, v (equation (5)), and vertical, w (equation (6)), directions; and eddy diffusion coefficients across, K_z (equation (7)), and along, K_σ (equation (8)), isopycnal surfaces.

[16] To a first-order approximation the change in carbonate ion concentration due to biological processes depends on the difference in the changes of Alk and DIC:

$$Alk - DIC \cong \left(\left[HCO_3^-\right] + 2\left[CO_3^{2-}\right] + \left[HBO_4^-\right]\right) - \left(\left[HCO_3^-\right] + \left[CO_3^{2-}\right]\right)$$
$$\Delta Alk - \Delta DIC \cong \Delta\left[CO_3^{2-}\right] \quad (2)$$

[17] The second relationship above is approximate primarily because it assumes the borate ion component of the alkalinity is constant, whereas it is a function of pH. *Emerson and Hedges* [2008, Table 4.8] demonstrate that during addition of CO_2 to surface waters about 60% of the carbonate ion change, $\Delta[CO_3^{2-}]$, expected from the above approximation is realized. Degassing of CO_2 because of the slight fCO_2 supersaturation in August and September (Figure 2) would cause a decrease in DIC and thus an increase in $[CO_3^{-2}]$. We show later, however, that gas exchange is only a small flux compared to organic carbon export determined from the oxygen mass balance in summer suggesting that gas exchange plays a minor role in the surface ocean carbon balance. If organic matter formation were the only process affecting the dissolved inorganic carbon in ocean surface waters during photosynthesis, DIC would decrease while Alk increased, increasing $[CO_3^{-2}]$. (During organic matter formation, $\Delta Alk \sim -(16/106) \times \Delta DIC$, assuming Redfield Ratio changes for N and organic C.) Surface water summertime decrease in DIC in the subarctic Pacific has been observed previously to be about -80 μmol kg^{-1} [*Wong et al.*, 2002]. If this change were due only to organic carbon production, with the resulting increase of 12 μeq kg^{-1} in alkalinity, it would result in an increase of the carbonate ion concentration of 58 μmol kg^{-1}, which is much greater than the observations in Figure 4.

[18] During $CaCO_3$ formation Alk decreases at twice the rate of DIC indicating that $CaCO_3$ precipitation alone would cause $[CO_3^{2-}]$ to decrease with time in surface waters. Qualitatively, fCO_2 and pH changes that result in the small, ~10 μmol kg^{-1}, $[CO_3^{2-}]$ increase during summer require formation of calcium carbonate and organic matter. In the following discussion we use a simple mass balance model to constrain the rates of $CaCO_3$ and organic matter formation.

4.2. The Rates of Organic Carbon and $CaCO_3$ Production

[19] *Emerson and Stump* [2010] determined net community organic carbon production during the summer of 2007 at Stn P using oxygen and nitrogen data along with a mixed-layer model. The model assumed a well-mixed surface layer of water that is open to gas exchange at the air-water interface and water exchange along and across isopycnals via advection and mixing (Figure 5). Since a detailed description of the model was presented previously, we review it only briefly here. The time rate of change of solute concentration, [C] (mol m^{-3}), in a mixed layer of depth h (m) is equal to the sum of air-water exchange, mixing and biological production.

$$h\,{}^{d[C]}\!/_{dt} = F_{A-W} + E + A_v + A_z + M_z + M_\sigma + J_C \quad (3)$$

Terms on the right hand side are: air-water gas exchange, $F_{A\text{-}W}$ (mol m^{-2} d^{-1}); entrainment due to mixed layer deepening, E; horizontal advection in the mixed layer, A_v; vertical exchange, either by upwelling, A_z, or mixing along and across density surfaces, M_z and $M\sigma$, respectively; and finally biological production, J_C. Each term for the physical processes is the product of a mass transfer coefficient or

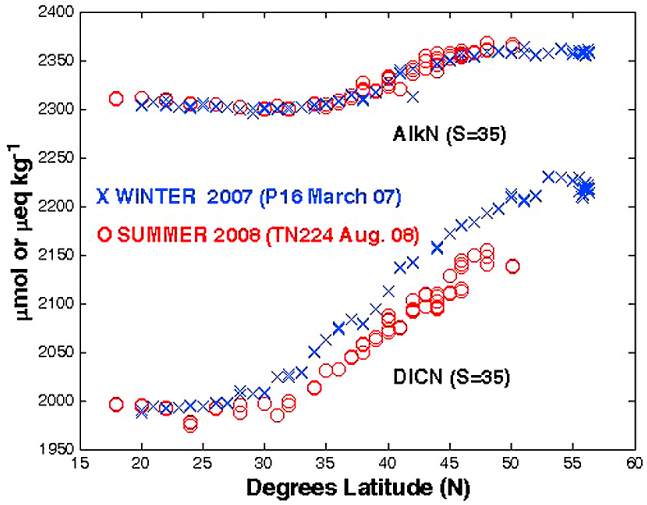

Figure 6. Surface concentrations of salinity-normalized alkalinity, AlkN (S = 35), and dissolved inorganic carbon, DICN (S = 35), in the northeast Pacific Ocean along 152°W. Data are presented for a winter cruise (P16, March, 2007) and a summer *Thompson* cruise (TN224, August/September 2008). The Clivar P16 data are available online, and the TN224 data are available from the authors.

mixing term and measured concentration or concentration gradients. The mass transfer coefficients and mixing terms are identified in Figure 5 and in the following equations. These quantities must be either measured or estimated from previous studies of physical processes in this region to determine the net biological carbon production, J_C.

[20] We solve equation (3) for DIC and Alk using O_2 and N_2-determined organic carbon production rates and a range of $CaCO_3$: OC production ratios. The terms of equation (3) that were most influential in controlling the summertime mass balance of O_2 and N_2 [*Emerson and Stump*, 2010] were the time rate of change and air-water gas transfer. Transport across the base of the mixed layer in summer by vertical advection and diffusion had minor influence. Local changes and air-water gas exchange are most important in the O_2 and N_2 mass balance because residence times of these gases with respect to air-sea exchange are relatively short: on the order of a few weeks to a month. This is not the case for dissolved inorganic carbon because the $[CO_2]$ gas is only a small component of the DIC in the mixed layer, and its residence time with respect to gas exchange is about 10 times that for oxygen and nitrogen. Local concentration changes of dissolved inorganic carbon and alkalinity are more influenced by mixing and advection than are O_2 and N_2, thus processes occurring in the greater subarctic north Pacific have more influence in the DIC and Alk mass balances. In the following paragraphs we briefly describe how each of the terms on the right side of equation (3) and the coefficients in Figure 5 were evaluated.

[21] The air water exchange term is normally separated into a diffusive flux, G (mol m^{-2} d^{-1}) and a bubble flux, B. The first is characterized by the mass transfer coefficient for gas exchange, k_C (m d^{-1}), multiplied by the difference in concentration of the gas in the mixed layer and that at saturation equilibrium with the atmosphere, $[C^{sat}]$.

$$F = G + B = k_C\{[CO_2] - [CO_2{}^{sat}]\} + V_{inj}\ X_C \qquad (4)$$

The air injection mechanism of bubble processes is parameterized by a mass transfer coefficient, V_{inj}, and the mole fraction of gas C in the atmosphere, X_C [e.g., *Hamme and Emerson*, 2006]. While bubble processes have a large influence on the gas exchange of insoluble gases like O_2 and N_2, they are not very important for the more soluble CO_2, and they are ignored here. The concentrations of dissolved CO_2 in the mixed layer and the value in equilibrium with the atmosphere ($[CO_2]$ and $[CO_2^{sat}]$) are calculated from the ocean and atmosphere fCO_2 data in Figure 2 using the solubility of CO_2 in seawater. The mass transfer coefficient, k_C, is dependent on the physical properties of the gas and solute via the Schmidt number, $S_C = (\nu/D)$, where ν (cm^2 s^{-1}) is the kinematic viscosity of the liquid and D (cm^2 s^{-1}) the molecular diffusion coefficient of the gas (see *Emerson and Hedges* [2008, chap. 9] for more details). The mass transfer coefficient has been correlated with wind speed in surface ocean purposeful tracer release experiments. We determine the mass transfer coefficient normalized to k_{CO2} at 20°C and S = 35 using the relationship to wind speed presented by *Nightingale et al.* [2000].

[22] Entrainment is active only when the mixed layer deepens in the fall and winter. Since we interpret the data only through September, this term is of little importance till the very latter part of the period of interest when concentrations below the mixed layer are incorporated while the mixed layer deepens.

[23] Ekman transport is assumed to dominate the advective flow in the mixed layer, h, which is about 30 m deep during most of the summer.

$$A_v = u\left(d[C]/dx\right)h + v\left(d[C]/dy\right)h \qquad (5)$$

Here, u and v (m d^{-1}) are the zonal and meridional components of surface currents. Ekman transport at Stn P is greater in winter than summer because of the variability in wind speed [*Roden*, 1977; *Ayers and Lozier*, 2010]. Winds are mainly to the east resulting in a southward vector of velocity that reaches values of ~0.1 m s^{-1} in the wintertime. (See results from the global ocean data assimilation System, http://ferret.pmel.noaa.gov/NVODS). We consider the southward component of the surface transport to be the most important because both meridional currents and concentration gradients are strongest. Both atmospheric wind and surface ocean current velocities were measured on the mooring in 2007 (data not presented). The southward component of the surface currents during the period of June to October 2007 was variable and small averaging essentially zero from 5 m depth measurements and 0.01 m s^{-1} from Ekman transport calculations. We use advection velocities that incorporate this range of measurements in the sensitivity analysis described below.

[24] Mixed layer concentration gradients of salinity-normalized alkalinity and dissolved inorganic carbon, AlkN and DICN, from both TN224 and CLIVAR P16 (Figure 6) indicate essentially no meridional gradient in AlkN north of

the subarctic-subtropical boundary, but a strong gradient in DIC which decreases to the south. Because curvature in the horizontal gradient is difficult to quantify from this data, we assume two extreme cases for horizontal advection of DIC. The minimum influence of meridional advection is represented by no divergence of flux at 50°N: the advective flux from the north equals that to the south. In the other extreme we assume no horizontal gradient north of 50°N so that meridional advection along the gradient south of Stn P would lower DICN without influencing AlkN causing a positive $\Delta Alk - \Delta DIC$, and hence an increase in $[CO_3^{2-}]$.

[25] Vertical advection across the base of the summer mixed layer is described by:

$$A_z = w\left(d[C]/dz\right)\Delta z \quad (6)$$

where w (m d^{-1}) is the upwelling velocity, and Δz represents the depth scale for vertical transport which we take to be the mixed layer depth. The high end of the range of vertical advection velocities calculated previously for this region is on the order of 1×10^{-6} m s^{-1} (*Tabata* [1961] and *Sasai and Ikeda* [2003], $w \sim 0.1$ m d^{-1}). These values are dominated by winter time upwelling and the value we determine from satellite wind stress curl patterns during the summer of 2007 is 100 times smaller and negligible in the transport balance.

[26] Vertical mixing across the base of the mixed layer is depicted as:

$$M_z = K_z\left(d[C]/dz\right) \quad (7)$$

where K_z (m^2 s^{-1}) is the vertical eddy diffusion coefficient (see Figure 5). Diapycnal mixing processes are difficult to evaluate, but are potentially important because of the strong gradient in DIC between the surface mixed layer and the region below. (From the data in Figure 3, the DIC difference between 25 and 75 m depth in August of 2008 was ~50 μmol kg^{-1}, whereas the gradient in Alk was negligible.) A minimum value for the vertical eddy diffusion coefficient is that estimated within the thermocline by microstructure measurements [*Gregg*, 1989] and measured by tracer release experiments [e.g., *Ledwell et al.*, 1998], $0.1–0.2 \times 10^{-4}$ m^2 s^{-1}. However, *Large et al.* [1986] showed that during storms, diffusive mixing across the base of the mixed layer at Stn P can be characterized by eddy diffusion coefficients up to one hundred times this value over short periods of time. We assume $K_z = 0.1 \times 10^{-4}$ m^2 s^{-1} is a lower limit and solve for values that are three times and ten times greater to determine the sensitivity to diapycnal mixing.

[27] Transport along density surfaces in the subarctic Pacific is also a vertical exchange because the depth of the density horizons representing the base of the winter mixed layer at Stn P (50°N) ($\sigma_\theta \sim 26.2$) plunges to ~200 m at 40°N and ~400 m at 30°N. Mixing along isopycnal surfaces is described by the diffusion equation:

$$M_\sigma = K_\sigma\left(d[C]/dl\right) \quad (8)$$

where l is the distance along the isopycnal surface and K_σ (m^2 s^{-1}) is the isopycnal eddy diffusion coefficient. This process connects the mixed layer in winter and water below the mixed layer in summer with deeper thermocline waters to the south. Isopycnal mixing does not play a role in the summertime mass balance of the mixed layer because it is isolated by thermal stratification. However, as we shall see, it is an important process balancing biological removal of $CaCO_3$ on an annual basis.

[28] We calculate the change in Alk and DIC in the mixed layer at Stn P using the same mass transfer coefficients employed to constrain the O_2 and N_2 mass balance [*Emerson and Stump*, 2010]. The value of the net biological oxygen production was transformed to net organic carbon production and DIC decrease using a $\Delta C/\Delta O_2$ ratio of −1/1.45 [*Hedges et al.*, 2002]. Initial alkalinity and DIC in the mixed layer are given values near those measured at 152°N (Figure 3) but adjusted to exactly match the fCO_2 and pH measured at Stn P in June 2007. Equation (3) is stepped forward in time and the fCO_2 and pH are recalculated by the chemical equilibrium equations after each time step. The process is completed for ratios of calcium carbonate to organic carbon export rates of, $CaCO_3$: OC = 0.0, 0.5 and 1.0, and for the range of advection and diapycnal eddy diffusion discussed above. Net biological organic carbon production rates determined from O_2 and N_2 mass balance are relatively insensitive (±20%) to this range of mixing parameters.

[29] Results of the calculations are presented in Figure 7 and Table 1. The top three panels of Figure 7 are solutions for a diapycnal eddy diffusion coefficient of 0.1×10^{-4} m^2 s^{-1}. The bottom three solutions are the changes derived for an eddy diffusion coefficient three times this value. In order to match the observed fCO_2 and pH with low K_z (Figure 7, Case I), it is necessary to have a $CaCO_3$: OC ratio of at least 0.5. No production of $CaCO_3$ results in fCO_2 and pH trends less than those observed and a value of $CaCO_3$: OC = 1.0 creates trends in the correct sense but too extreme. Increasing the vertical eddy diffusion coefficient (Figure 7, Case II) makes it possible to match the fCO_2 and pH data using a $CaCO_3$: OC = 0.0, but we show in the following paragraph describing the results in Table 1 that this case violates other constraints.

[30] The sensitivity analysis in Table 1 compares results from different model runs with observed changes in summertime fCO_2 and pH (as in Figure 7) and also with expected changes in Alk and DIC. Expected alkalinity changes are determined from carbonate equilibrium with fCO_2 and pH. Because calculated alkalinity is susceptible to small errors in these measurements, we assume a wide range of acceptable alkalinity change in the row labeled "Measured Values" of Table 1. The constraint for summertime change in DIC is taken from previous measurements during the summertime in the eastern subarctic Pacific of ~−80 μmol kg^{-1} over a period of 2 years (1995–1997 [*Wong et al.*, 2002]) from container ship crossings from Asia to Western North America. Because these data are from an earlier time, we assume an acceptable value for 2007 to be somewhere in the range of $\Delta DIC = -(50–100)$ μmol kg^{-1}.

[31] The sensitivity analysis was carried out for a southward component of advection in the surface layer of 0 and 0.01 m s^{-1}; however, only the results for v = 0.01 m s^{-1} are presented in Figure 7 and Table 1 because horizontal advection of this magnitude made little difference in the predicted changes. Bold values of the "Model Results" in

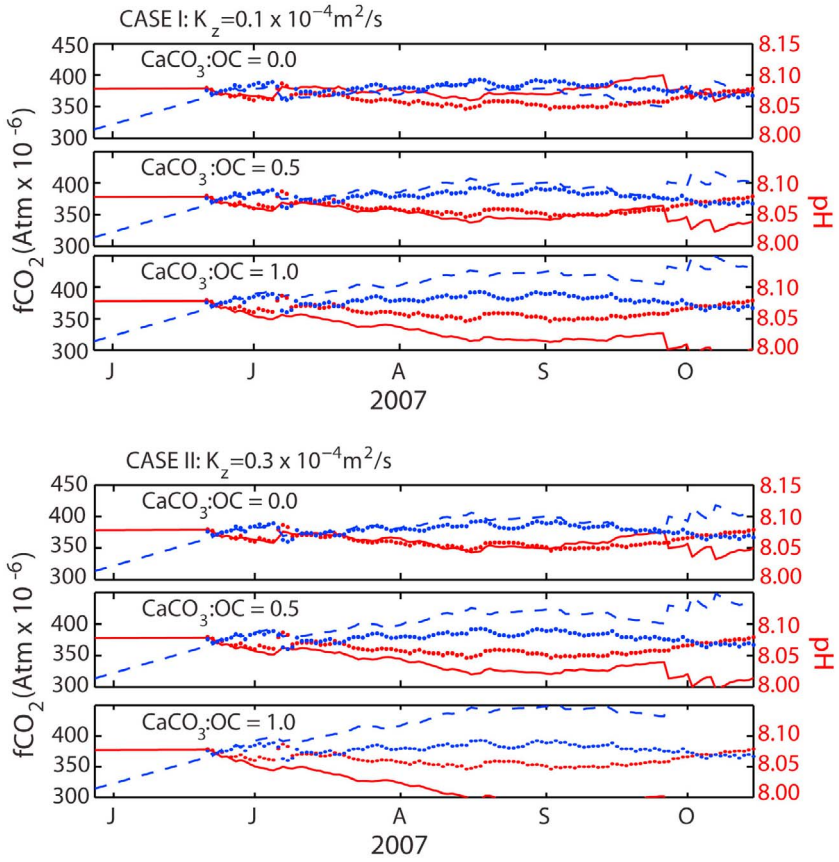

Figure 7. Comparison of model predictions and observations of fCO_2 and pH as a function of month in 2007. Thin lines are the model estimates, and solid symbols represent the data. Model solutions are for an advective velocity, v, of 0.01 m s^{-1} and $CaCO_3$:OC values of 0.0, 0.5, and 1.0. The top three panels (CASE 1) are solutions in which the vertical eddy diffusion coefficient is the minimum value of K_z = 0.1×10^{-4} m^2 s^{-1}. The bottom three panels (CASE II) are solutions in which the vertical eddy diffusion coefficient is $K_z = 0.3 \times 10^{-4}$ m^2 s^{-1}.

Table 1 are those that fall within the range of "Measured Values" at the top. We evaluate acceptable ratios of $CaCO_3$: OC by a process of elimination: (a) The high value for the eddy diffusion coefficient of 1.0×10^{-4} m^2 s^{-1} creates both fCO_2 and pH changes that are much too extreme for all $CaCO_3$: OC ratios indicating that the diapycnal diffusion rate is strongly constrained by the steep depth gradient of DIC accompanied by almost no gradient in alkalinity. (b) Another clear incompatibility between model and measurements is that the $CaCO_3$: OC ratio = 1 and $K_z = 0.3 \times 10^{-4}$ m^2 s^{-1} produces an fCO_2 change that is too large. (c) At the other extreme the combination of $CaCO_3$: OC = 0 and

Table 1. Sensitivity Analysis of Modeled and Measured Summertime Changes, Δ, in fCO_2, pH, DIC, and Alk to the Range of Values for the Vertical Eddy Diffusion Coefficient, K_z, and the Calcium Carbonate to Organic Carbon Rain Ratio, $CaCO_3$[a]

$K_z \times 10^4$ (m^2 s^{-1})	$CaCO_3$/OC	ΔpH	ΔfCO_2 (ppm)	ΔDIC (μmol kg^{-1})	ΔAlk (μeq kg^{-1})
		Measured Values			
		−(0.01–0.03)	5–15	−(50–100)	−(25–100)
		Model Results			
0.1	0.0	0.02	−11	−36	6
	0.5	−0.00	**12**	**−62**	**−36**
	1.0	**−0.03**	37	**−90**	**−77**
0.3	0.0	**−0.01**	22	−22	7
	0.5	−0.04	48	**−49**	**−42**
	1.0	−0.07	76	**−84**	**−84**
1.0	0.0	−0.08	110	9	6
	0.5	−0.11	142	−19	**−36**
	1.0	−0.14	179	**−47**	**−77**

[a]OC discussed in the text. "Model values" given in bold font are within the range of the "measured values."

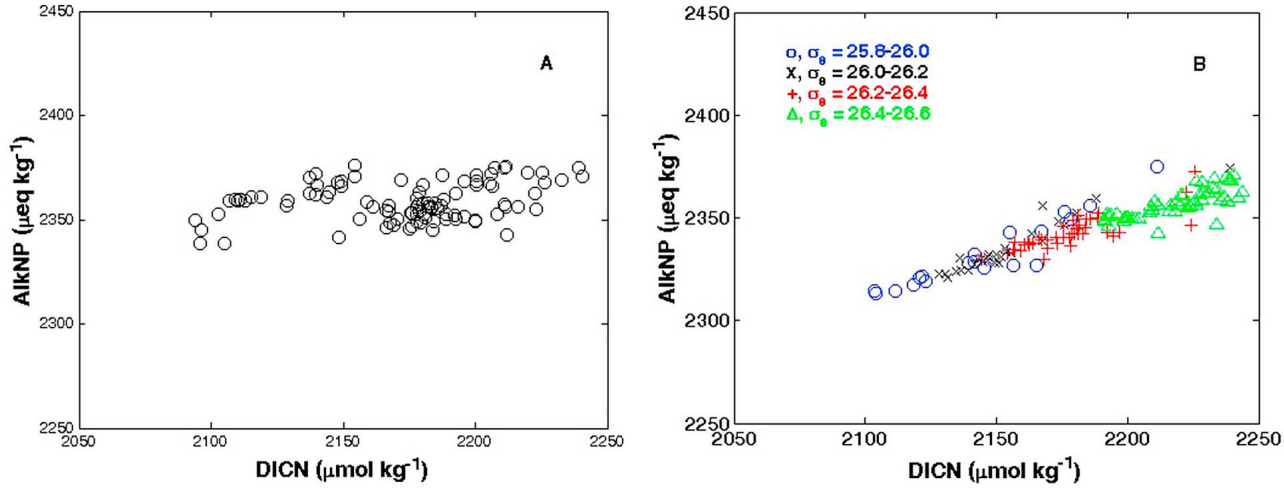

Figure 8. Salinity-normalized potential alkalinity, AlkNP, versus salinity-normalized dissolved inorganic carbon, DICN. Data are from *Thompson* cruise TN224 (see Figure 3). (a) Concentrations in the upper 200 m of subarctic Pacific waters (145°W–152°W and 43°N–50°N). The winter mixed layer depth in this location is ~110 m. (b) Concentrations along density surfaces between 30° and 50°N in the upper ~500 m along 152°W.

$K_z = 0.1 \times 10^{-4}$ creates fCO_2 and pH changes in the opposite sense to those measured.

[32] We have now eliminated all but the 2–5th rows in Table 1. All these scenarios are within or close to the acceptable range of fCO_2 and pH change. Only the case for $CaCO_3$: OC = 0 and $K_z = 0.3 \times 10^{-4}$ m^2 s^{-1} clearly violates acceptable trends in DIC and Alk. The predicted alkalinity change for this scenario is positive, which is in dramatic contrast to the change required for chemical equilibrium with fCO_2 and pH (−25 to −100 μeq kg^{-1}). Also, the calculated ΔDIC of −23 μmol kg^{-1} is much smaller for this case than previously measured summertime changes of −(50–100) μmol kg^{-1}.

[33] In order to meet the constraints of the temporal changes of the carbonate system as determined by time series measurements of fCO_2, pH and previous measurements of DIC change in summer our model suggests that the $CaCO_3$: OC ratio must be on the order of 0.5. Acceptable values are between 0.5 and 1.0 for $K_z = 0.1 \times 10^{-4}$ m^2 s^{-1} and <0.5 for $K_z = 0.3 \times 10^{-4}$ m^2 s^{-1}. Combining the $CaCO_3$: OC ratio with the organic carbon production rate of 17 mmol m^{-2} d^{-1} results in a flux of $CaCO_3$ from the surface ocean in this region of ~8 mmol m^{-2} d^{-1}.

4.3. Alkalinity Mass Balance for the Upper Ocean in the Subtropical Pacific

[34] If the $CaCO_3$ is being produced at a rate that is about half of that of organic carbon in the subarctic Pacific in summer, what are the processes that supply alkalinity to the surface waters? Horizontal fluxes via surface water transport are negligible in this area of the subarctic Pacific because of small gradients both meridionally (Figure 6) and zonally (data not shown). Vertical transport of DIC and Alkalinity have been used to estimate the $CaCO_3$: Organic C production rate ratio of 0.05–0.1 for the world's ocean with the Northeast Pacific near Stn P in this range [*Sarmiento et al.*, 2002; *Jin et al.*, 2006]. These values are much smaller than the ratio suggested here for the summer of 2007 ($CaCO_3$: OC ~ 0.5). Insight into the importance of the different pathways of DIC and Alk supply to the surface waters of the subarctic N. Pacific is gained by comparing salinity-normalized dissolved inorganic carbon, DICN, and potential alkalinity AlkNP. (Potential alkalinity is the sum of alkalinity and nitrate concentrations, Alk + [NO_3^-], which normalizes the observed alkalinity for changes due to organic matter degradation.) A plot of this type for the upper 200 m in the subarctic Pacific Ocean indicates very little vertical gradient in alkalinity across the depth of the winter mixed layer, 120m, resulting in a ΔAlkNP/ΔDICN ratio of only ~0.1 (Figure 8a). In a one dimensional steady state system a ratio of 0.1 will accommodate a $CaCO_3$: OC rain ratio of ~0.13, which is consistent with the results of *Sarmiento et al.* [2002] and *Jin et al.* [2006], but not with our derived $CaCO_3$: OC rain ratio.

[35] Another potential transport mechanism to subarctic Pacific surface waters is transport along constant density surfaces. Density horizons that outcrop in the subarctic Pacific in winter (σ_θ = 26.0–26.4) plunge into the subtropical thermocline to the south (Figure 3). A plot of AlkPN versus DICN along these isopycnal surfaces (Figure 8b) yields a ΔAlkPN: ΔDICN ratio of about 0.4 rather than 0.1. If the pathway for exchange of carbonate parameters between the surface waters in the subarctic ocean and deeper waters is along isopycnal surfaces, the source of alkalinity for $CaCO_3$ formation is much greater.

[36] The alkalinity gradient along an isopycnal surface that crops out in the subarctic Pacific in winter necessary to supply the $CaCO_3$ fluxes reported here by along-isopycnal eddy diffusion can be determined from equation (8):

$$F_{alk} = K_\sigma(\Delta Alk/\Delta l)$$

Using a distance, Δl, of 20° latitude (50°N and 30°N; $\Delta l = 2.22 \times 10^6$ m), an along-isopycnal eddy diffusion coefficient

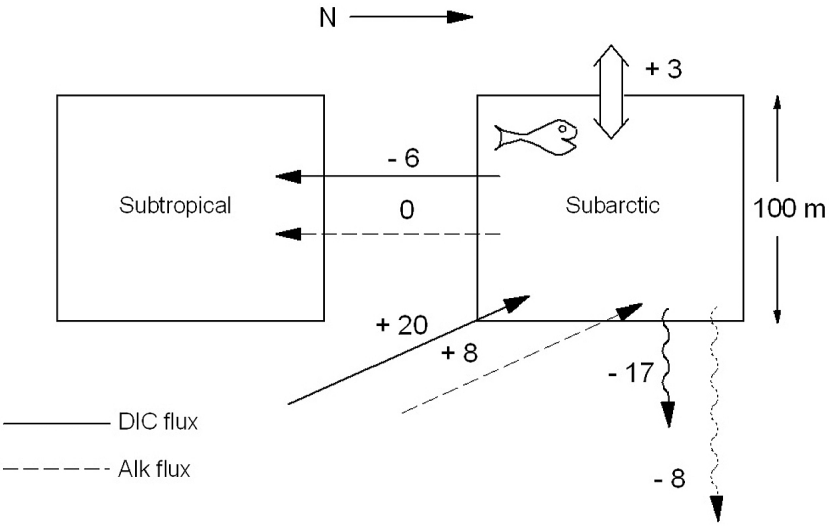

Figure 9. A schematic representation of DIC and Alk sources and sinks to, + (from, −), the subarctic Pacific Ocean surface waters. Solid lines indicate DIC fluxes, and dashed lines indicate alkalinity fluxes in mmol or meq m^{-2} d^{-1}. Values are determined from the following fluxes and flux ratios: The biological carbon flux from the euphotic zone = −17 mmol m^{-2} d^{-1} (O_2 and N_2 mass balance [*Emerson and Stump*, 2010]); the $CaCO_3$:OC of this biological flux = 0.5 (this paper); the isopycnal flux ratio AlkNP:DICN = 0.4 (Figure 8b); the annual gas exchange flux = + 3 mmol m^{-2} d^{-1} (see section 5); horizontal surface Ekman transport of Alk = 0, because there is no surface gradient (Figure 6); and the horizontal DIC flux, −6, is determined by difference (see section 5).

K_σ = 1000 m^2 s^{-1} [*Ledwell et al.*, 1998; *Gananadesikan et al.*, 2002] and an alkalinity flux necessary to maintain a $CaCO_3$ flux of 8 mmol m^{-2} d^{-1} (F_{alk} = 16 meq m^2 d^{-1}) results in an alkalinity increase of only about one microequivalent over a distance of 20 degrees latitude. Measured changes (Figure 3) are many times this value indicating the potential of this source, even if it operates only for a very brief time each year when the isopycnals crop out in the winter mixed layer.

5. Conclusions

[37] Organic carbon export from surface waters in the eastern subarctic Pacific at Stn P is estimated to be 17 mmol C m^{-2} d^{-1} in the summer of 2007 based on in situ, time series measurements of oxygen and nitrogen gas mass balance (2.5 mol C m^{-2} yr^{-1} assuming 150 days of productivity [*Emerson and Stump*, 2010]). Here we use in situ fCO_2 and pH data from the same period to constrain the $CaCO_3$: OC production ratio to be about 0.5. Together these results suggest a $CaCO_3$ production of ~8 mmol m^{-2} d^{-1} in summer with very little production in winter, which results in an annual flux of 1.2 mol $CaCO_3$ m^{-2} yr^{-1}. The $CaCO_3$ production rate is rate is similar to that determined using estimates of seasonal change of DIC and Alk from regressions to T and NO_3^- [*Lee*, 2001] for the four grid points surrounding Stn P (0.9 ± 0.1 mol C m^{-2} yr^{-1}, Kitack Lee, personal communication, 2009). It is also within the range of values determined in this area during the summer using in vitro methods [*Lipsen et al.*, 2007].

[38] Sediment trap collections at 200 m at Sta P have a $CaCO_3$: OC molar ratio of between 0.25 and 0.5 in summer [*Wong et al.*, 1999; Timothy et al., submitted manuscript, 2011]; however, the sediment trap absolute fluxes of both OC and $CaCO_3$ are far less than those predicted here. Mean values for summertime sediment trap fluxes at 200 m over many years of observations were ~2.5 and ~0.8 mmol m^2 d^{-1} compared to our estimates of 17 and 8 mmol C m^{-2} d^{-1}. Part of this difference can be attributed to the rapid decrease in particle flux between the mixed layer and 200 m. Three short-term deployments of free-floating sediment traps in 1987, 88 and 93 [*Wong et al.*, 1999] resulted in decreases between 50 and 200 m in organic and inorganic carbon fluxes of ~3 times and 1.5 times, respectively. Thus, extrapolating the climatological sediment trap fluxes at 200 m to shallower depths approaches organic carbon fluxes that are about half of the values determined here, but the 50 m $CaCO_3$ flux is still ~7 times lower than our suggested value. It is not unusual for sediment trap fluxes to under estimate particle fluxes particularly during high flux events [*Benitez-Nelson et al.*, 2001], which would be associated with $CaCO_3$ formation. It is also possible that we cannot assume the earlier trap fluxes are representative of the conditions of our observations, particularly since $CaCO_3$ production appears to be much more of an irregular process than net organic carbon export. *Wong et al.* [2002] observed that DIC summertime drawdown in the north Pacific was a regular and repeatable while alkalinity changes show no consistent seasonal change.

[39] A $CaCO_3$: OC production ratio of 0.5 suggested here is about 5 times the value determined for this area by *Sarmiento et al.* [2002] and *Jin et al.* [2006] based on vertical gradients of Alk and DIC. Part of this difference may be that our measurements span a period of only one season and are local while estimates derived from climatological data are annual averages and more basin-wide in scale. We also demonstrate that transport along isopycnal surfaces that

outcrop in the north Pacific is the most important flux pathway supplying alkalinity to the euphotic zone to accommodate $CaCO_3$ export determined from our in situ measurements. Interpreting vertical gradients of Alk and DIC can give misleading results about the importance of $CaCO_3$ export locally.

[40] Using the fluxes reported here we construct a regional carbon flux balance (Figure 9) that assumes a steady state over a period of at least several years. The net biological organic matter production of 17 mol m^{-2} d^{-1} (2.5 mol C m^{-2} yr^{-1}) determined from the in situ O_2 and N_2 measurements combined with a $CaCO_3$: OC ratio of 0.5 require an alkalinity export of ~8 meq m^{-2} d^{-1} (1.2 mol $CaCO_3$ m^{-2} yr^{-1}). The alkalinity that leaves the euphotic zone by biological processes must be balanced by an isopycnal flux because of the very small gradients in normalized potential alkalinity in both surface waters (Figure 6) and vertically (Figure 8a). A flux of 8 meq m^{-2} d^{-1} of alkalinity to the upper ocean along isopycnal surfaces with an AlkNP: DICN ratio of 0.4 implies an additional source of DIC of ~20 mmol $m^{-2}d^{-1}$. The DIC mass balance is closed by a net export of 3 mmol m^{-2} d^{-1} out of the subarctic upper ocean via the combined fluxes across the air-water interface and surface water transport to the subtropical ocean.

[41] The importance of gas exchange in the carbon cycle in the northeast subarctic Pacific is determined using equation (4) and the fCO_2 data (Figure 2). To a first approximation surface waters were slightly supersaturated in the summer of 2007, and undersaturated by an average of 15 ppm in winter. Using mean gas exchange mass transfer coefficients for CO_2 in summer and winter of 3 and 6 m d^{-1}, respectively [see *Emerson and Stump*, 2010] along with the fCO_2 data results in a mean annual flux from the atmosphere to the ocean of ~3 mmol m^{-2} d^{-1}. This additional source to the subarctic mixed layer means that the flux of DIC to the south via surface ocean advection must be about 6 mmol C m^{-2} d^{-1}. *Sasai and Ikeda* [2003] modeled the observed DIC distribution in the North Pacific Ocean using an ocean GCM and climatological distributions of DIC. Their biological organic carbon export values were about half those suggested here and the Ekman transport to the subtropics was less, but the same fluxes dominated the balance.

[42] The source of alkalinity to the subarctic Pacific Ocean is from depths of 300–500 m in the subtropical ocean. The carbonate ion concentration necessary for thermodynamic saturation with respect to aragonite in these waters is about 80 μmol kg^{-1} (Figure 3). Density contours that surface above 100 m in the subarctic Pacific in winter (σ_θ = 26.0–26.4, Figure 3) are supersaturated and the degree of supersaturation actually increases as the isopycnal surfaces deepen to the south. At steady state there must be a source of alkalinity from $CaCO_3$ dissolution to balance the flux of particulate $CaCO_3$ from the surface waters. From a thermodynamic point of view, there is no reason to expect $CaCO_3$ dissolution on density surfaces that supply alkalinity to the subarctic surface waters. The alkalinity source must come from either dissolution within undersaturated microenvironments of supersaturated water primarily in the subtropical ocean or via mixing of waters containing dissolution-derived alkalinity from depth [*Friis et al.*, 2006].

[43] **Acknowledgments.** Ship time for the mooring operations was provided by the P-Line Program of the Institute of Ocean Sciences (IOS), Sidney, B. C., Canada. The authors thank Marie Robert, the Captain and crew of the CCGS *Tully*, and the IOS administration for collaboration and maintaining an excellent time series program. Charles Stump, Patrick A'Hearn, and David Zimmerman provided outstanding technical help during the deployment and recovery of the mooring. We would like to thank David Timothy of IOS for showing us a preliminary version of the sediment trap paper compilation and for helpful discussions about the comparison of their data with our observations. The research was funded by NSF grants OCE-0628663 (S.E. and M.C.) and OCE-0836807 (M.D. and S.C.).

References

Archer, D., S. Emerson, T. Powell, and C. S. Wong (1993), Numerical hindcasting of sea surface pCO_2 at Weathership Station Papa, *Prog. Oceanogr.*, *32*, 319–351, doi:10.1016/0079-6611(93)90019-A.

Armstrong, R. A., C. Lee, J. I. Hedges, S. Honjo, and S. Wakeham (2002), A new, mechanistic model for organic carbon fluxes in the ocean based on the quantitative association of POC with ballast minerals, *Deep Sea Res., Part II*, *49*, 210–236.

Ayers, J. M., and M. S. Lozier (2010), Physical controls on the seasonal migration of the North Pacific transition zone chlorophyll front, *J. Geophys. Res.*, *115*, C05001, doi:10.1029/2009JC005596.

Balch, W., D. Drapeau, B. Bowler, and E. Booth (2007), Prediction of pelagic calcification rates using satellite measurements, *Deep Sea Res., Part II*, *54*, 478–495, doi:10.1016/j.dsr2.2006.12.006.

Benitez-Nelson, C., K. O. Buesseler, D. M. Karl, and J. Andrews (2001), A time-series of particulate matter export in the North Pacific subtropical gyre based on ^{234}Th:^{238}U disequilibrium, *Deep Sea Res.*, *48*, 2595–2611, doi:10.1016/S0967-0637(01)00032-2.

Berelson, W. M., W. M. Balch, R. Najjar, R. A. Feely, C. Sabine, and K. Lee (2007), Relating estimates of $CaCO_3$ production, export, and dissolution in the water column to measurements of $CaCO_3$ rain into sediment traps and dissolution on the sea floor: A revised global carbonate budget, *Global Biogeochem. Cycles*, *21*, GB1024, doi:10.1029/2006GB002803.

Broecker, W. S., and T. H. Peng (1982), *Tracers in the Sea*, Eldigio Press, Palisades, N. Y.

Cullison Gray, S. E., M. D. DeGrandpre, T. M. Moore, T. R. Martz, G. E. Friederich, and K. S. Johnson (2011), Applications of in situ pH measurements for inorganic carbon calculations, *Mar. Chem.*, *124*, 82–90, doi:10.1016/j.marchem.2011.2.005.

Dickson, A. G., J. D. Afghan, and G. C. Anderson (2003), References materials for oceanic CO_2 analysis: 2. A method for the certification of total alkalinity, *Mar. Chem.*, *80*, 185–197, doi:10.1016/S0304-4203(02)00133-0.

Emerson, S., and J. H. Hedges (2008), *Chemical Oceanography and the Carbon Cycle*, Cambridge Univ. Press, Cambridge, U. K., doi:10.1017/CBO9780511793202.

Emerson, S., and C. Stump (2010), Net biological oxygen production in the ocean: II. Remote in situ measurements of O_2 and N_2 in subarctic Pacific surface waters, *Deep Sea Res., Part I*, doi:10.1016/j.dsr.2010.06.001.

Favorite, F., J. Dodimead, and K. Nash (1976), Oceanography of the subarctic Pacific region, 1960–1971, *Int. North Pac. Fish Comm. Bull.*, *33*, 187 pp.

Feely, R. A., et al. (2002), In situ calcium carbonate dissolution in the Pacific Ocean, *Global Biogeochem. Cycles*, *16*(4), 1144, doi:10.1029/2002GB001866.

Friederich, G. E., P. G. Brewer, R. Herlein, and F. P. Chavez (1995), Measurement of sea surface partial pressure of CO_2 from a moored buoy, *Deep Sea Res., Part I*, *42*, 1175–1186, doi:10.1016/0967-0637(95)00044-7.

Friis, K., R. G. Najjar, M. J. Follows and S. Dutkiewicz (2006), Possible overestimation of shallow-depth calcium carbonate dissolution in the ocean, *Global Biogeochem. Cycles*, *20*, GB4019, doi:10.1029/2006GB002727.

Gananadesikan, A., R. D. Slater, N. Gruber, and J. L. Sarmiento (2002), Oceanic vertical exchange and new production: A comparison between models and observations, *Deep Sea Res., Part II*, *49*, 363–401.

Gregg, M. C. (1989), Scaling turbulent dissipation in the thermocline, *J. Geophys. Res.*, *94*, 9686–9698, doi:10.1029/JC094iC07p09686.

Hales, B., and S. Emerson (1997), Calcite dissolution in sediments of the Ceara Rise: In situ measurements of porewater O_2, pH and CO_2, *Geochim. Cosmochim. Acta*, *61*, 501–514, doi:10.1016/S0016-7037(96)00366-3.

Hamme, R. C., and S. R. Emerson (2006), Constraining bubble dynamics and mixing with dissolved gases: Implications for productivity measurements and oxygen mass balance, *J. Mar. Res.*, *64*, 73–95, doi:10.1357/002224006776412322.

Hedges, J. I., J. A. Baldock, Y. Gelinas, C. Lee, M. L. Peterson, and S. G. Wakeham (2002), The biochemical and elemental compositions

of marine plankton: An NMR perspective, *Mar. Chem.*, *78*, 47–63, doi:10.1016/S0304-4203(02)00009-9.

Honjo, S., J. Dymond, R. Collier, and S. J. Manganini (1995), Export production of particles to the interior of the equatorial Pacific Ocean during 1992 EqPac experiment, *Deep Sea Res., Part II*, *42*, 831–870, doi:10.1016/0967-0645(95)00034-N.

Howard, E., S. Emerson, S. Bushinsky, and C. Stump (2010), The role of net community biological production in air-sea carbon fluxes at the North Pacific subarctic-subtropical transition region, *Limnol. Oceanogr.*, *55*, 2585–2596, doi:10.4319/lo.2010.55.6.2585.

Jahnke, R. A., D. B. Craven, and J.-F. Gaillard (1994), The influence of organic matter diagenesis on $CaCO_3$ dissolution at the deep-sea floor, *Geochim. Cosmochim. Acta*, *58*, 2799–2809, doi:10.1016/0016-7037(94)90115-5.

Jin, X., N. Gruber, J. P. Dunne, J. L. Sarmiento, and R. A. Armstrong (2006), Diagnosing the contribution of phytoplankton functional groups to the production and export of particulate organic carbon, $CaCO_3$, and opal from global nutrient alkalinity distributions, *Global Biogeochem. Cycles*, *20*, GB2015, doi:10.1029/2005GB002532.

Johnson, K. M., et al. (1998), Coulometric total carbon dioxide analysis for marine studies: Assessment of the quality of total inorganic carbon measurements made during the U.S. Indian Ocean CO_2 survey 1994–1996, *Mar. Chem.*, *63*, 21–37, doi:10.1016/S0304-4203(98)00048-6.

Klaas, C. and D. E. Archer (2002), Association of sinking organic matter with various types of mineral ballast in the deep sea: Implications for the rain ratio, *Global Biogeochem. Cycles*, *16*(4), 1116, doi:10.1029/2001GB001765.

Kwon, E. Y., F. Primeau, and J. L. Sarmiento (2009), The impact of remineralization depth on the air-sea carbon balance, *Nat. Geosci.*, *2*, 630–635, doi:10.1038/ngeo612.

Large, W. G., J. C. McWilliams, and P. P. Niller (1986), Upper ocean thermal response to strong autumnal forcing of the northeast Pacific, *J. Phys. Oceanogr.*, *16*, 1524–1550, doi:10.1175/1520-0485(1986)016<1524:UOTRTS>2.0.CO;2.

Large, W. G., J. C. McWilliams, and S. C. Doney (1994), Oceanic vertical mixing: A review and a model with a nonlocal boundary layer parameterization, *Rev. Geophys.*, *32*, 363–403, doi:10.1029/94RG01872.

Ledwell, J. R., A. J. Wilson, and C. S. Law (1998), Mixing of a tracer in the pycnocline, *J. Geophys. Res.*, *103*, 21,499–21,529, doi:10.1029/98JC01738.

Lee, K. (2001), Global net community production estimated from the annual cycle of surface water total dissolved inorganic carbon, *Limnol. Oceanogr.*, *46*, 1287–1297, doi:10.4319/lo.2001.46.6.1287.

Lee, K., L. T. Tong, F. J. Millero, C. L. Sabine, A. G. Dickson, C. Goyet, G-H. Park, R. Wanninkhof, R. A. Feely and R. M. Key (2006), Global relationships of total alkalinity with salinity and temperature in surface waters of the world's oceans, *Geophys. Res. Lett.*, *33*, L19605, doi:10.1029/2006GL027207.

Lipsen, M. S., D. W. Crawford, J. Gower, and P. J. Harrison (2007), Spatial and temporal variability in coccolithophore abundance in the production of PIC and POC in the NE subarctic Pacific during El Niño 1998, La Niña 1999 and 2000, *Prog. Oceanogr.*, *75*, 304–325, doi:10.1016/j.pocean.2007.08.004.

Lueker, T. J., A. G. Dickson, and C.D. Keeling (2000), Ocean pCO_2 calculated from dissolved inorganic carbon, alkalinity and the equations for K_1 and K_2: Validation based on laboratory measurements of CO_2 in gas and seawater at equilibrium, *Mar. Chem.*, *70*, 105–119, doi:10.1016/S0304-4203(00)00022-0.

Martz, T. R., J. J. Carr, C. R. French, and M. D. DeGrandpre (2003), A submersible autonomous sensor for spectrophotometric pH measurements of natural waters, *Anal. Chem.*, *75*, 1844–1850, doi:10.1021/ac020568l.

Mehrbach, C., H. Culberson, J. E. Hawley, and R. M. Pytkowicz (1973), Measurement of the apparent dissociation constants of carbonic acid in seawater at atmospheric pressure, *Limnol. Oceanogr.*, *18*, 897–907, doi:10.4319/lo.1973.18.6.0897.

Millero, F. J., et al. (1998), Total alkalinity measurements in the in Indian Ocean during the WOCE Hydrographic Program CO_2 survey cruises 1994–1996, *Mar. Chem.*, *63*, 9–20, doi:10.1016/S0304-4203(98)00043-7.

Moore, J. K., S. C. Doney, J. A. Kleypas, D. M. Glover, and I. Y. Fung (2002), An intermediate complexity marine ecosystem model for the global domain, *Deep Sea Res., Part II*, *49*(1–3), 403–462.

Mucci, A. (1983), The solubility of calcite and aragonite in seawater at various salinities, temperatures, and one atmosphere total pressure, *Am. J. Sci.*, *283*, 780–799, doi:10.2475/ajs.283.7.780.

Nightingale, P. D., G. Malin, C. S. Law, A. J. Watson, P. S. Liss, M. I. Liddicoat, J. Boutin, and R. C. Upstill-Goddard (2000), In situ evaluation of air-sea gas exchange parameterizations using novel conservative and volatile tracers, *Global Biogeochem. Cycles*, *14*, 373–387, doi:10.1029/1999GB900091.

Roden, G. (1977), Ocean subarctic fronts of the central Pacific: Structure of the response to atmospheric forcing, *J. Phys. Oceanogr.*, *7*, 761–778, doi:10.1175/1520-0485(1977)007<0761:OSFOTC>2.0.CO;2.

Sarmiento, J. L., and N. Gruber (2007), *Ocean Biogeochemical Dynamics*, Princeton Univ. Press, Princeton, N. J.

Sarmiento, R. L., J. Dunne, A. Gnanadesikan, R. M. Key, K. Matsumoto and R. Slater (2002), A new estimate of the $CaCO_3$ to organic carbon export ratio, *Global Biogeochem. Cycles*, *16*(4), 1107, doi:10.1029/2002GB001919.

Sasai, Y., and M. Ikeda (2003), A model study for the carbon cycle in the upper layer of the North Pacific, *Mar. Chem.*, *81*, 71–88.

Seidel, M. P., M. D. DeGrandpre, and A. G. Dickson (2008), A sensor for in situ indicator-based measurements of seawater pH, *Mar. Chem.*, *109*, 18–28, doi:10.1016/j.marchem.2007.11.013.

Tabata, S. (1961), Temporal changes of salinity, temperature and dissolved oxygen content of the water at Station "P" in the northeast Pacific Ocean, and some of their determining factors, *J. Fish. Res. Bd. Can.*, *18*, 1073–1124, doi:10.1139/f61-066.

Weiss, R. F. (1974), Carbon dioxide in water and seawater, the solubility of an non-ideal gas, *Mar. Chem.*, *2*, 203–215, doi:10.1016/0304-4203(74)90015-2.

Wong, C. S., and Y.-H. Chan (1991), Temporal variations in the partial pressure and flux of CO_2 at ocean station P in the subarctic northeast Pacific Ocean, *Tellus, Ser. B*, *43*, 206–223.

Wong, C. S., F. A. Whitney, D. W. Crawford, K. Iseki, R. J. Matear, W. K. Johnson, J. S. Page, and D. Timothy (1999), Seasonal and interannual variability in particle fluxes of carbon, nitrogen and silicon from time series sediment traps at Ocean Station P, 1982–1993: Relationship to changes in subarctic primary productivity, *Deep Sea Res., Part II*, *46*, 2735–2760, doi:10.1016/S0967-0645(99)00082-X.

Wong, C. S., D. Waser, Y. Nojiri, F. A. Whitney, J. Page, and J. Zeng (2002), Seasonal cycles of nutrients and dissolved inorganic carbon at high and mid latitudes in the North Pacific Ocean during the Skaugran cruises: Determination of new production and nutrient uptake ratios, *Deep Sea Res., Part II*, *49*, 5317–5338, doi:10.1016/S0967-0645(02)00193-5.

Yamanaka, Y., and E. Tajika (1996), The role of the vertical fluxes of particulate organic matter and calcite in the oceanic carbon cycle: Studies using an ocean biogeochemical general circulation model, *Global Biogeochem. Cycles*, *10*, 361–382, doi:10.1029/96GB00634.

M. F. Cronin, R. Feely, and C. Sabine, Pacific Marine Environmental Laboratory, NOAA, Seattle, WA 98115, USA.

S. E. Cullison Gray and M. DeGrandpre, Department of Chemistry and Biochemistry, University of Montana, Missoula, MT 59812, USA.

S. Emerson, School of Oceanography, University of Washington, Seattle, WA 98195, USA. (emerson@u.washington.edu)